Bollettino di Geofisica Teorica ed Applicata Vol. 53, n. 4, pp. 385-401; December 2012
DOI 10.4430/bgta0046

In search of new imaging for historical earthquakes: a new geophysical survey offshore western Calabria (southern Tyrrhenian Sea, Italy)

M.F. Loreto[1], F. Zgur[1], L. Facchin[1], U. Fracassi[2], F. Pettenati[1], I. Tomini[1], M. Burca[1], P. Diviacco[1], C. Sauli[1], G. Cossarini[1], C. De Vittor[1], D. Sandron[1] and the Explora team of technicians[1]

[1] *Istituto Nazionale di Oceanografia e di Geofisica Sperimentale, Sgonico (TS), Italy*
[2] *Istituto Nazionale di Geofisica e Vulcanologia, Rome, Italy*

(Received: April 1, 2011; accepted: November 22, 2011)

ABSTRACT During the summer of 2010 we carried out a survey to acquire a multidisciplinary dataset within the Gulf of Sant'Eufemia (south-eastern Tyrrhenian sea, Italy), with the aim of studying the active tectonics affecting the region, including that potentially responsible for key, elusive earthquakes such as the to-date unexplained September 8, 1905 (M_W 7-7.5) earthquake. The data here analyzed highlight the presence of several tectonic and morphologic features characterizing the investigated area. We have recognized the Angitola Channel, a deep and wide canyon showing a straight trend in its coastward segment, and a meandering trend in the seaward segment. Based on morpho-structural elements, we maintain that the Angitola Channel could be tectonically controlled. Moreover, several gravitational instabilities as slumps and slides affect the flanks of the morpho-structural high, detected offshore Capo Vaticano. Very high resolution seismic data have unveiled the presence of numerous fluid escape features and several mud volcanoes straddling the sector from the coastline to seawards.

Key words: 1905 earthquake, active tectonics, mud volcanoes, Gulf of Sant'Eufemia.

1. Introduction

Calabria is one of the Italian regions with the largest number of catastrophic ($M_w > 7$) earthquakes, mainly located in a relatively narrow landstrip. Among the several ones, the event that occurred on the night of September 8, 1905 in southern Calabria is probably the strongest, according to the estimated M_W 7.5 [Michelini *et al*. (2006); macroseismic M_W, derived from intensity data, is ~7.0: see Gruppo di Lavoro CPTI04 (2004)]. This earthquake generated a tsunami (see Piatanesi and Tinti, 2002) that, while not catastrophic, was observed both in the open sea and along the coast bordering the Gulf of Sant'Eufemia, on the western termination of the Catanzaro Straits. This earthquake claimed 557 casualties, more than 2000 injured. About 300,000 people were left homeless. Although this event severely devastated a wide area, its age and the poor documentation have long caused it to go relatively overlooked and not fully constrained in terms of magnitude and epicentral location. To begin with: did this earthquake occur offshore or onshore? Dubious epicentral locations (see stars in Fig. 1), which go hand in

© 2012 – OGS

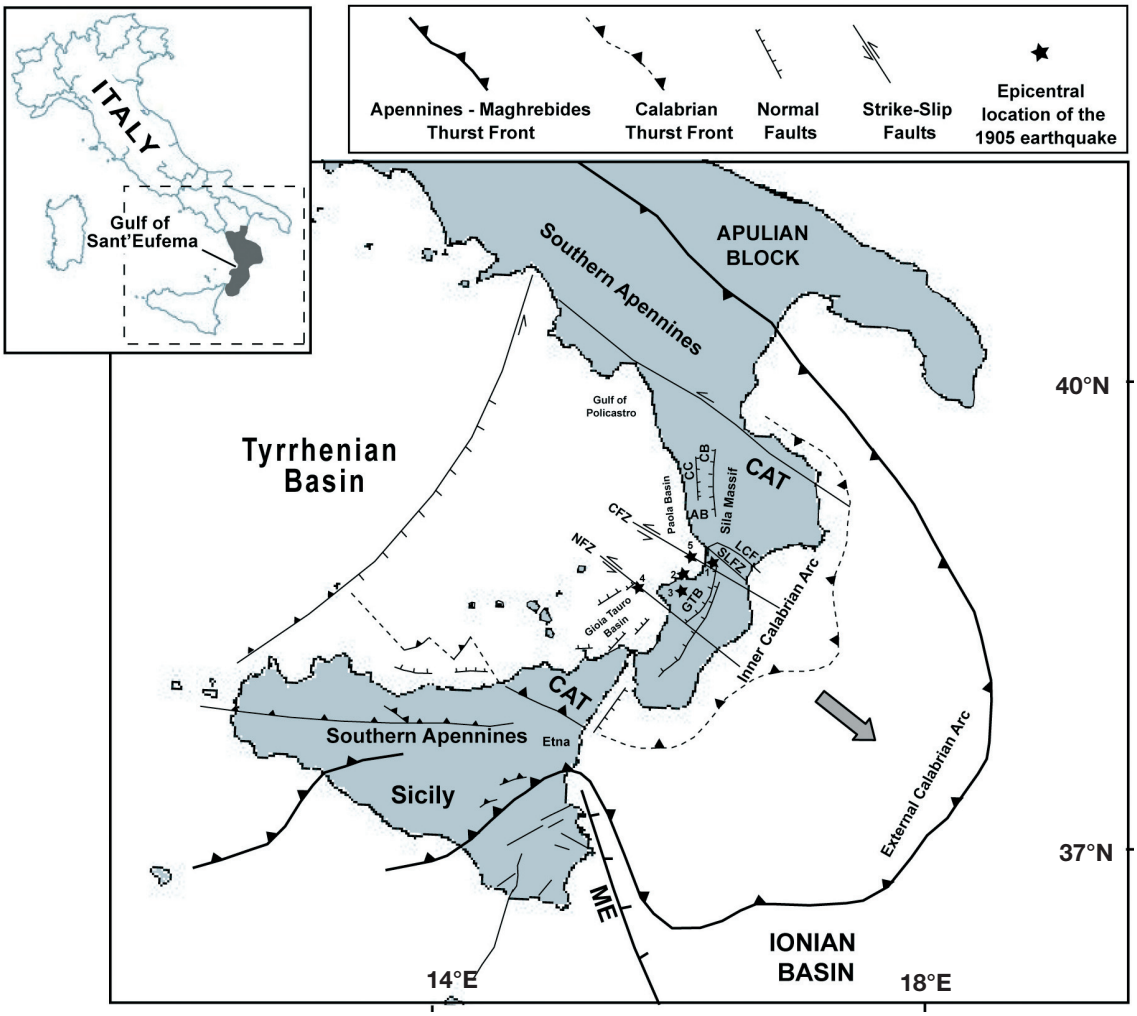

Fig. 1 - Structural sketch-map of the southern Apennines and Calabrian Arc, simplified by Van Dijk *et al*. (2000) and Catalano and Sulli (2006). Abbreviations are as follows: CB = Crati Basin; CC = Catena Costiera; AB = Amantea Basin; NFZ = Nicotera Fault Zone; LCF = Lamezia-Catanzaro Fault; SLFZ = Soverato-Lamezia Fault Zone; CFZ = Catanzaro Fault Zone by Finetti and Del Ben (1986); GTB = Catanzaro Basin; CAT = Calabrian Arc Terranes; ME = Malta Escarpment. Stars indicate the epicentral locations for the September 8, 1905 earthquake suggested by several authors: 1 Rizzo (1906); 2 Camassi and Stucchi (1997); 3 Boschi *et al*. (1995); 4 Michelini *et al*. (2006); 5 Riuscetti and Schick (1974). Location of the study area is in the inset to the upper left.

hand with uncertain M_W estimates [see some reasoning on this subject in Fracassi *et al*. (2012) and references therein]. For similar reasons, it is not straightforward to associate this earthquake with a positively identified seismogenic source (i.e., Tiberti *et al*., 2006; Tertulliani and Cucci, 2009).

To address these issues and to improve the knowledge concerning the seismogenic potential of the region, we performed a targeted geophysical, oceanographic and bio-geochemical survey in the Gulf of Sant'Eufemia (south-eastern Tyrrhenian Sea, southern Italy). The aim of the project was: a) to study the active tectonics of the region, and b) gain insight into tectonic features that

could help to identify the potential seismogenic source of the September 8, 1905 earthquake.

To support the geophysical survey, during the survey planning we performed an inversion of the 1905 macroseismic dataset using the kinematic function (KF: Pettenati and Sirovich, 2007). This procedure uses as input the intensity distribution of the macroseismic field.

2. Geological and geodynamic setting

The remarkably complex geology of Calabria has been thoroughly studied by numerous authors in the past decades [see a good synthesis in Amodio-Morelli *et al*. (1976)]. During the early Miocene, the Calabrian Arc Terrains (CAT in Fig. 1) were located close to the Corsica-Sardinia block (Bigi *et al*., 1992; Bonardi *et al*., 2001). During the middle-late Miocene these tectonic domains drifted until juxtaposition with the southern Apennines (Alvarez *et al*., 1974; Bonardi *et al.*, 2001; Mattei *et al*., 2002). The CAT units are unconformably overlain by Tertiary sedimentary sequences, deposited in different tectonic provinces of the Calabrian Arc. Moreover, Miocene to Quaternary deposits, outcropping along the Tyrrhenian side, are interpreted as part of a back–arc extensional basin. These deposits are associated with the opening and the spreading of the southern Tyrrhenian Sea (Sartori, 1990; Mattei *et al*., 2002; Cifelli *et al*., 2007). During Quaternary times an extensional phase, to-date active, contributed to the deepening of the southern Tyrrhenian Basin (the Marsili Basin) and to the uplift of the Calabrian Arc (recorded by a regional unconformity).

Extensional and uplift phases could be related to the warping of the oceanic slab (Sartori, 2003). Moreover, continental deposits, in-land of the Gulf of Sant'Eufemia, according to Tansi *et al*. (2007) have experienced recent intense strike-slip tectonics (Fig. 1). In this area, major strike-slip fault systems, that apparently segment the Calabrian Arc, are well documented, including the Soverato-Lamezia Fault Zone and the Nicotera Fault Zone (Tansi *et al*., 2007). The activity of large fault systems since the Middle Pleistocene, particularly in the Squillace area, is also documented by Del Ben *et al*. (2008).

If one concentrates on the recent geological evolution of this region, complexities all disappear. The long and multi-history geology of Calabria (see Van Dijk *et al*., 2000), the remarkably high relief energy, the very high uplift rates, and obviously the subduction processes, all concur to somehow mask the late Quaternary evolution of this region. Unlike the regional strike-slip tectonics, possibly active, that has been imaged in the Catanzaro Straits (Tansi *et al*., 2007), tectonic features witnessing the on-land activity east of the Gulf of Sant'Eufemia are not easy to identify, at least in the sector from Lamezia Terme to Vibo Valentia. Various geomorphological studies, however, shed light on a number of significant landscape features. To the east and NE, Tansi *et al*. (2007) have shown Late-Pleistocene-Holocene alluvial fans adjacent to the Lamezia-Catanzaro Fault (LCF in Fig. 1) that separates the uplands of the Sila massif (to the north) from the lowlands of the Catanzaro Straits (to the south), where these authors also identified Middle Pliocene-Middle Pleistocene deposits on the flanks of the Amato River valley, i.e., the alluvial plain in the western sector of the Catanzaro Straits.

To the south, the Gulf of Sant'Eufemia is bounded by the Capo Vaticano promontory, a regional morpho-tectonic feature that separates the Catanzaro Straits (to the north) from the Gioia Tauro plain (to the south). Tortorici *et al*. (2003) have explored the terrace flight that can be found

on the entire promontory due to the widespread uplift affecting this and several other sectors of Calabria (see Pirazzoli *et al*., 1997). Based on their interpretation and on the kinematics they have identified, Tortorici *et al*. (2003) maintain that the youngest (lowermost) terraces that encircle the promontory are as young as 60 kyrs. Some remnants can be found on the coast north of Vibo Valentia, bordering our study area.

3. New data

During the scientific survey, from August 28 to September 14, 2010 on board of the R/V OGS-Explora, we acquired 330 km of MultiChannel Seismic (MCS) data, 2223 km of sub-bottom Chirp profiles, 2231 km^2 of high resolution morpho-bathymetric data, Multibeam-derived backscatter data, 12 geological (gravity cores) and biological samples, the latter sampled at the top of the cores and stored at -20°C. Finally, we performed 12 CTD (Conductivity-Temperature-Depth) and 10 water samples measurements, using Niskin bottle samplers. The sampled water at different depth is used to derive the DIC (Dissolved Inorganic Carbon), H_2S (Hydrogen Sulfide), Ph and salinity content. Moreover, we acquired ADCP (Acoustic Doppler Current Profiler) and thermo-salinographer data during the entire cruise. The geophysical dataset and the location of samples are reported on the high-resolution morpho-bathymetric map shown in Fig. 2.

3.1. Geophysical data

A high resolution morpho-bathymetric image of the seafloor (Fig. 2) was obtained by using the two hull mounted MultiBeam echosounders (MBES): a Reson Seabat 8111 (100 kHz) and a Reson Seabat 8150 (12 kHz). The Seabat 8111 reaches the maximum swath width (7.4 times the water depth) when working in less than 150 m of water, and was used in waters up to 400 m deep. The Seabat 8150 works in a water depth range of 500 - 12000 m with a maximum swath width of 4.5 times the water depth. All data were acquired with 40% of overlap.

We acquired 2223 km of very high resolution (Chirp) acoustic data during the MultiBeam survey. The Chirp data image in detail the shallower sedimentary cover from the seafloor to a maximum depth of 75 m, this assuming a constant sound speed of about 1550 m/s within the shallowest sediments.

Based on the preliminary results of the morpho-bathymetric and high resolution acoustic surveys, we then acquired a tight grid of intermediate resolution MCS sections (red lines in Fig. 2). In Table 1, the acquisition parameters of the MCS data are reported.

On-board, we performed early real-time quality control on all MCS data acquired. The pre-processing of seismic data consisted in: data reformatting; trace editing, amplitude recovery, conversions from SP (Shot Point) to CMP (Common Mid Point) – applied using the SORT algorithm, velocity analysis every 400 CMPs, NMO (Normal Move Out) correction, and brute stack. Later, a more accurate processing of the seismic dataset was performed until to the time migration.

In this paper, the preliminary results only related to geophysical data analysis are discussed, highlighting some very interesting structural and morphological features. The integration of results stemming from bio-geochemical, oceanographic and sedimentary data is in progress. The overall aim of this analysis is to investigate possible multiple/concomitant signals of geothermal activities in different domains (water and sediment).

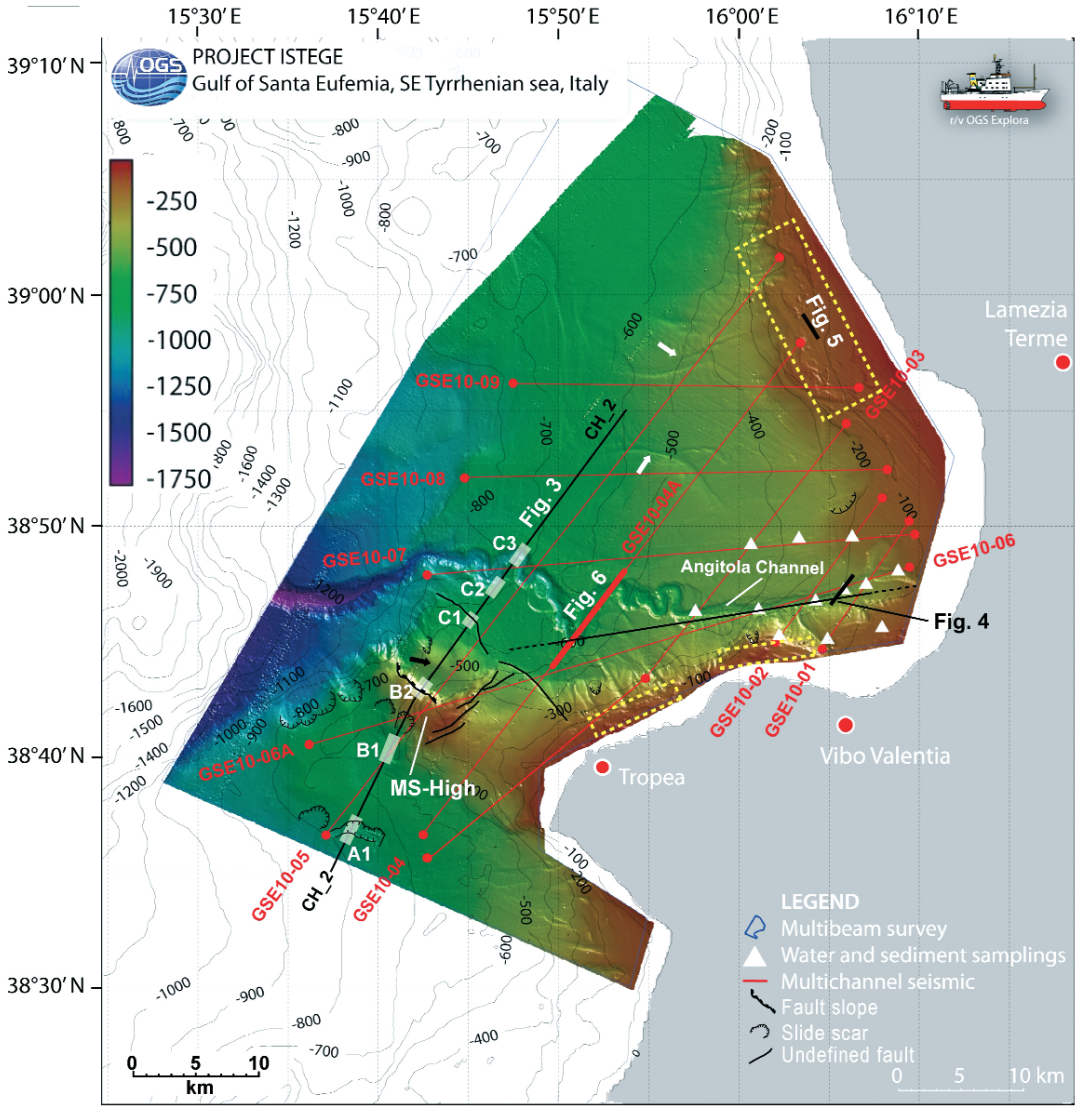

Fig. 2 - Shaded relief of the high resolution morpho-bathymetric raw data of the investigated area. Yellow dashed rectangle indicates the area of the mud volcanoes and fluid escapes occurrence. The MCS dataset location is reported with red lines, while the discussed segment with thick red line is highlighted. White triangles indicate the locations of the bio-geochemical samples. Black lines indicate the locations of the Chirp profiles. Transparent rectangles are the boxes point out in Fig. 3. White thick arrows indicate the rivers incisions (see legend for the morpho-structural features inferred from the geophysical data analyzed and on the map reported).

4. Results

4.1. Morpho-bathymetric features

The high resolution bathymetric data (Fig. 2) allowed us to define the morphology of the Gulf of Sant'Eufemia in detail. The key morphologic element that we recognized is a large submarine canyon, already known in the literature as Angitola Channel (Gamberi and Marani, 2004). In the internal part of the Gulf, the channel shows a straight trend, ca. ENE-WSW oriented for about 20 km.

Table 1 - Acquisition parameters of the MCS data.

ACQUISTION PARAMETERS					
SOURCE		**STREAMER**		**RECORDING**	
Model	GI-GUN Sercel	Model	Sercel Seal	Model	Sercel Seal
Total volume	about 8 l	Lenght	1500 m	Sampling rate	1.0 ms
Shot interval	25 m	Chan. number	120	Leng. record	8 s
Depth	4 m ± 0.5 m	Chan. Interval	12.5 m	LC filter	3 Hz (LC);
Pressure	140 atm.	Depth	5 m ± 0.5 m	HC filter	Anti-alias
		Min. Offset	50 m	Auxiliary Chan.	Ch.12
		Max Offset	1550 m		
		Coverage	30		

At about 420 m depth the channel starts to meander, a feature also confirmed by several generations of terraces. We believe that this is a typical channel-canyon system similar to those identified south of the Capo Vaticano promontory (Gamberi *et al*., 2011). At about 900 m depth, the channel, cutting the continental margin, strongly deepens and widens. In particular, the channel shows an axial depth that increases from about 3 m, close to the coast, to ca. 300 m at the external slope. In the internal slope, several erosive features and some gravitational instability were detected. They affect mainly the southern side slope, between Vibo Valentia and Tropea, and the northernmost part of the gulf. Similar features can be recognized also south of the Capo Vaticano promontory.

Offshore Tropea, we identified a NW-SE oriented morpho-structural high (MS-High in Fig. 2), that appears to be the underwater portion of the Capo Vaticano promontory. The top of the MS-High shows elongate NE-SW trending, morphological features, against which a NW-SE oriented steep slope ends (see Fig. 2). Between the northern slope of the Gulf of Sant'Eufemia and the Angitola channel, bathymetric data show few noteworthy morphological features, like channel incisions (see white arrows in Fig. 2). Between the coastline and the border of the internal slope, the seafloor shows small wrinkles. This trend of the shelf is recognized along both the northern and the southern side of the gulf (see yellow boxes in Fig. 2). Finally, around the MS-High and south of it, we recognized several slide scars that affect the seafloor (indicated with comb lines in Fig. 2). North of the MS-High, we identified few other, slide scars.

4.2. Shallow features imaged by Chirp data

Fig. 3 shows Chirp profile Ch_2 that crosses both the Angitola Channel and the MS-High (see location in Fig. 2). South of the MS-High, everywhere sediments are apparently undeformed and well stratified, except in two areas. The first one, defined as Gas Escape Zone, shows that the current sediments abruptly end and that they are vertically shifted (see white arrows in Fig. 3A). This area is composed by two major discontinuities and by a minor one in-between, which a very small vertical shift could be associated with. Moreover, we recognized two gas plumes above such discontinuities (see box A1 in Fig. 3A). The second deformed zone (see box B1 in Fig. 3B), likely corresponding to the Nicotera Fault Zone (Fig. 1), is represented by reflectors affected by

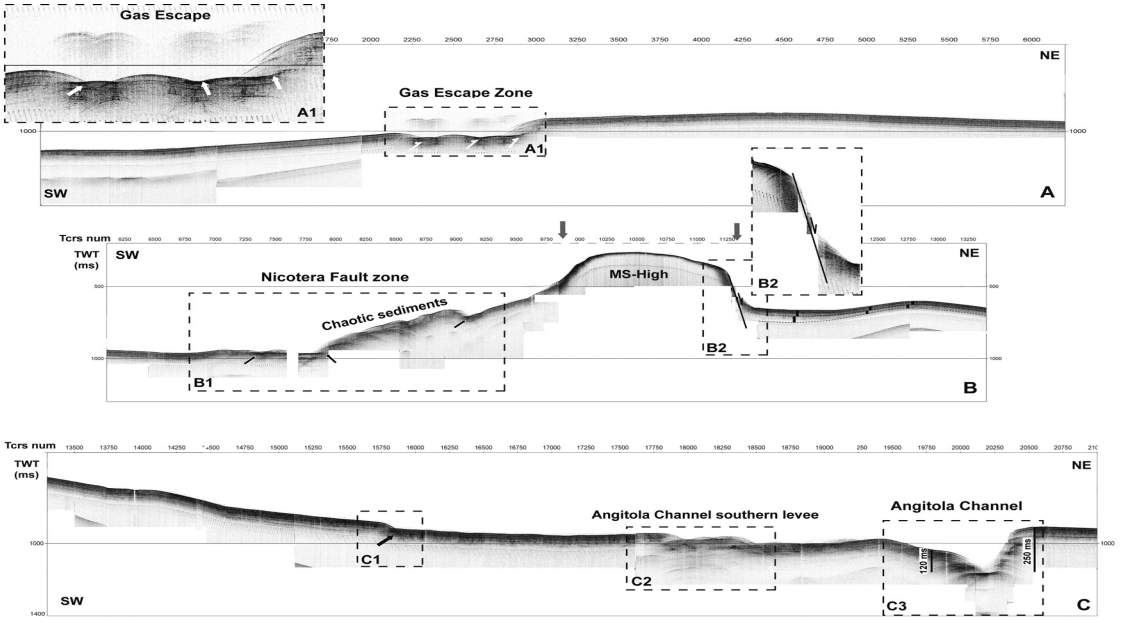

Fig. 3 - Chirp profile CH_2 (location in Fig. 2). White arrows indicate sediments discontinuities affecting the gas escape zone (A1). Main discontinuities are indicated with black thick arrows (See B1 and C1). MS-High: Morpho-Structural Ridge. Dashed rectangles border the area affected by tectonics (A1, B1, B2, C1) and that concerning the Angitola Channel (C2 and C3).

diffractions, abrupt interruptions and loss of stratification, which we identified as chaotic sediments. Laterally, the chaotic features suddenly end (see black thick arrows) and the undisturbed stratification becomes the dominant character.

Between 9000 and 11500 (grey arrows in Fig. 3B), a morpho-structural high (MS-High) is present, whose top is characterized by reflectivity loss and reduction of signal penetration. The north-eastern side of the MS-High is represented by a very steep slope characterized by reflectivity loss and defocusing of the reflected energy at the seafloor (see box B2 in Fig. 3), that we believe to be controlled by a normal fault. This slope bounds well stratified sediments that, as indicated by thick black lines (Fig. 3B), thinly and gently rise northeastwards.

To the NE, we detected a deep incision on the seafloor, corresponding to the Angitola Channel (see box C3 in Fig. 3C). The northern levee shows a bathymetric jump of about 250 ms (corresponding to 187 m assuming a water velocity of 1500 m/s), while the southern levee shows a jump of 120 ms (i.e., 90 m). SW of the Angitola Channel, layered sediments are locally interrupted and affected by some diffractions. This area corresponds to the southern meander of the channel (see Fig. 2 and Box C2 in Fig. 3C). Between this meander and the MS-High, a small discontinuity is underlined by a minor shift of both seafloor and present-day sediments (see Box C1 in Fig. 3C).

Fig. 4 shows part of a Chirp line that we acquired across the Angitola Channel (see location in Fig. 2). Sediments are well stratified, with opposite dipping trend between the two sides; the reflectors are apparently more transparent along the south-western side if compared with those in

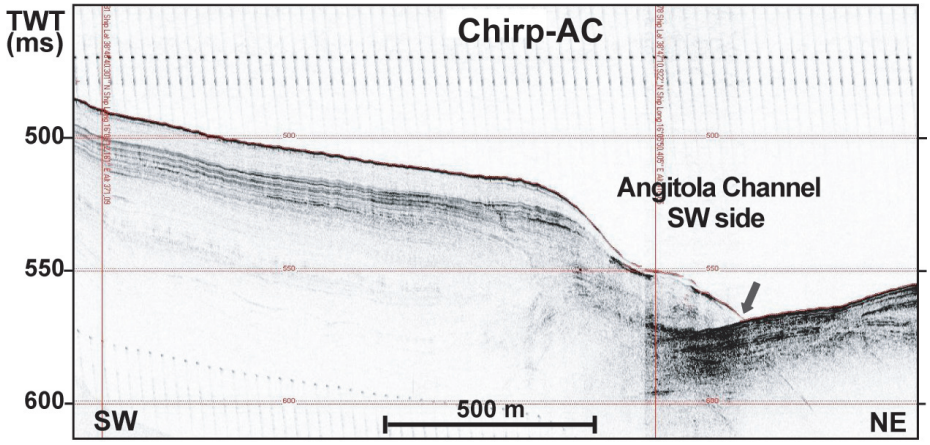

Fig. 4 - Chirp-AC profile acquired close to the inner part of the gulf trough the Angitola Channel incision (Fig. 2). Gray arrow indicates sediment deformation along the side of the channel.

the north-eastern side. The seafloor deepens northeastwards without discontinuity until the inception of the channel, where it results deformed (see gray thick arrow). Moreover, at the channel bed a chaotic and transparent body overlaps the layered sediments. At the north-eastern end of the cross section, the sediment reflectivity continues to be high but less clear. This sedimentary setting suggests a likely tectonic control of the channel trend and a gravity instability affecting the channel levee.

We identified several fluid escapes and mud volcanoes along the northern margin of the Gulf of Sant'Eufemia (Fig. 5); such features frequently affect the shallow sediments outcropping on the seafloor. Two sub-horizontal recent deposits (U1 and U2) overlay a well stratified and tilted one (U3). The U1 layers abruptly stop against the sides of a high that we interpret as a mud volcano. The top of the U3 deposit shows different depth (outlined by dashed lines). Finally, the U2 deposits are horizontally stratified although there is a loss of reflectivity close to the volcano, where a strong thickness variation is outlined by the black thick lines in Fig. 5. Moreover, we identified a chaotic deposit at the top of the U2 unit on the right side of the volcano (see arrow in Fig. 5). Considering the characteristics of the U3 unit, the origin of the mud volcano can be tentatively associated with fault activity, whose attitude and kinematics remain unclear.

4.3. Features imaged by MCS data

In Fig. 6 we show a portion of the GSE_4 seismic profile. This profile is SW-NE oriented, parallel to the coastline (Fig. 2), and crosscuts the Angitola Channel twice (see RiverBed 1 - RB1 and RiverBed 2 - RB2 in Fig. 6). The south-western levee of RB1 shows a morphological scarp about 200 ms high, corresponding to about 150 m. Sediments below RB1 show gentle folding (see black thick arrow) involving all deposits up to the top of the Miocene units. The latter is imaged by a high amplitude and continuous seismic reflector on which Plio-Quaternary, well stratified sediments, on-lap (see also Milia *et al.*, 2009; Pepe *et al.*, 2010). The Plio-Quaternary

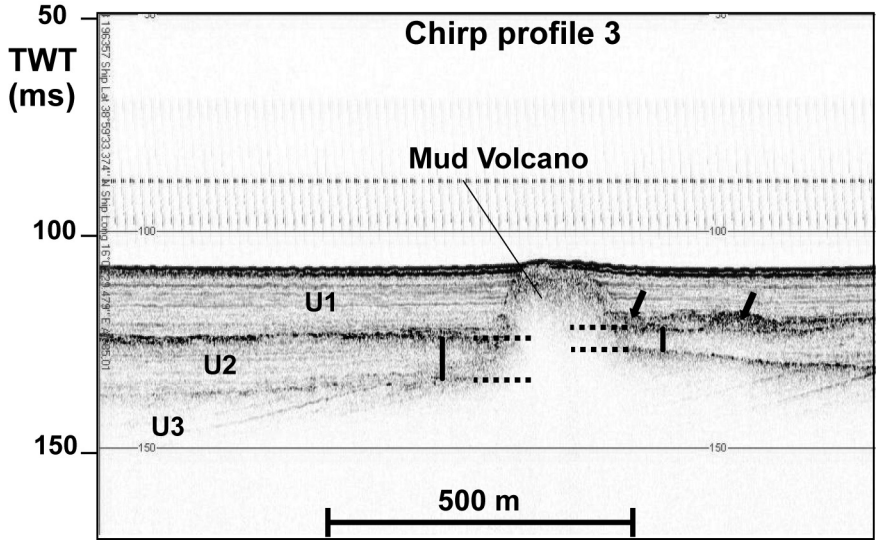

Fig. 5 - Chirp profile 3 acquired in the upper shelf along the northern side of the gulf (see location in Fig. 2). Three main sedimentary units are identified: U1 = Unit 1; U2 = Unit 2; and U3 = Unit 3. Black dashed lines indicate depth of both top of Unit 3 and Unit 2. Black thick lines indicate thickness of the Unit 2. A chaotic deposit is underlined by the black arrows.

units are well stratified, although showing a strong lateral thickness variation. The tectonics that likely affects the Miocene unit is outlined by discontinuities, reflectivity loss, and diffractions localized at its top (see white thick arrows in Fig. 6A). Close to RB2, the seafloor is shallower than on the south-western side; between RB1 and RB2 several bed-forms and seismic diffractions affect sediments (see gray thick arrows).

A map showing the top of the Miocene deposits (Fig. 7) highlights its key tectonic features. The 2D map was obtained interpolating the picking of the horizon depth (in TWT). Generally, the top of the Miocene deposits deepens seawards following the coast-line trend, although some anomalous features can be recognized. In particular, close to the coast the top of Miocene unit is deeper in than the surrounding area (see white arrow in Fig. 7); seawards, it rises of about 1 s (TWT; see black arrow) if compared with the central part of the gulf (see gray arrow).

5. Methodology of intensity inversion

Since the procedure applied in the present paper has been well documented in the literature [Sirovich (1996) and Pettenati and Sirovich (2003) for the KF model; Gentile *et al*. (2004) and Sirovich and Pettenati (2004) for the inversion method; Pettenati *et al.* (2005)], we will here only provide a brief description. The methodology is based on expressing the radiation from an earthquake in terms of the dimensionless values of a kinematic function KF based on the representation theorem (Aki and Richards, 1980): the method shows that displacement at a given point on the ground-surface far from the fault is proportional to the energy at the source. Here,

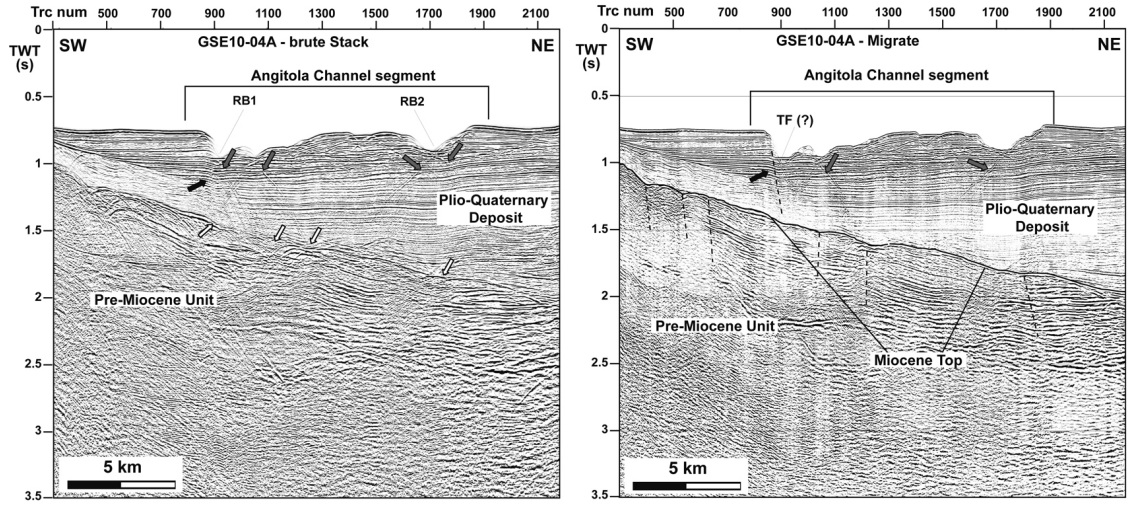

Fig. 6 - Part of seismic stack (a) and migrate (b) profile GSE_04 located in the central part of the gulf (see Fig. 1). The Angitola Channel is displayed, showing the RB1 – Riverbed 1 and RB2 – Riverbed 2. Grey thick arrows indicate shallow seismic diffractions. Black thick arrow indicates folded sediments. White thick arrows indicate seismic diffractions at the Miocene Top. Hypothesized faults are reported as dashed black lines on the migrate section. The likely transcurrent fault affecting the Angitola channel is reported as TF(?).

we stress that in the KF approach only the body wave radiation is considered. Therefore, the KF model is satisfactory at distances from the source as close as the order of the wavelength, while beyond 80-100 km the amplitudes of surface waves progressively prevail over those of body-waves.

The KF procedure is unable to discriminate between the results produced by mechanisms which differ by 180° in the rake angle, since in both cases the method returns the same radiation, only with reversed polarities. This ambiguity, which comes in addition to the classic one concerning affecting the focal mechanism solution between fault and auxiliary plane, may be solved only with additional geological information.

5.1. The inversion procedure

Due to the fact that the inversion of the KF is a non-linear problem, we used a Niching Genetic Algorithm (NGA). Genetic algorithms provide advantages in terms of global optimization and computational costs over other randomized search schemes (e.g., local optimization), which moreover easily could be biased by the starting conditions.

The NGA algorithm is based on routines from the library by Levine (1996). Briefly, this variant of normal genetic algorithm splits the population in subpopulations (demes) each evolving independently in the parameters hyperspace with objective function being the sum of the squared residuals, Σr_s^2 (r_s is the pseudo-intensity i calculated at each site, minus the intensity I observed at the same site). In this work, we used four demes each of 1,000 individuals (i.e., sources). Further details concerning the method can be found in Sirovich and Pettenati (2004) and in Gentile *et al*. (2004), while the error estimation of each parameter is described by Pettenati and

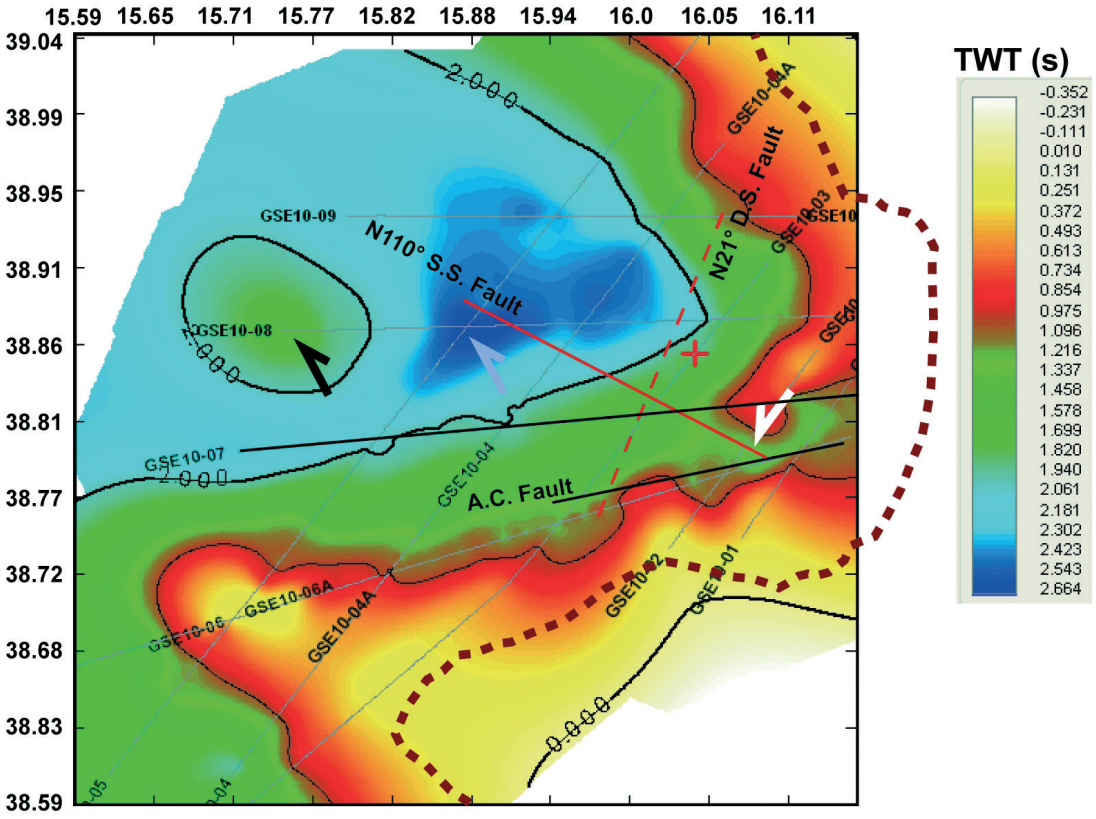

Fig. 7 - Interpolation map of the depth of the top of Miocene picked using the Kingdom software. The entire seismic dataset used is reported. The Angitola Channel Fault (A.C. Fault) is indicated with a solid black line. The solid red line indicates the N110° strike-slip fault, while the dashed red line shows the N21° normal fault. The arrows (white, black and grey) indicate unexpected trends of the top of Miocene. The coast line is reported as brown dashed line.

Sirovich (2007).

5.2. The September 8, 1905 earthquake inversion

In Fig. 8A intensity points from the data reported by Guidoboni *et al*. (2007) were interpolated by Natural Neighbor algorithm (Sirovich *et al*., 2002) within 80 km from the epicenter. In the dataset we deleted 5 data points considered outliers [for a similar example, see Pettenati and Sirovich (2003)]. Fig. 8A shows that the intensities distribution is not strongly homogeneous, and that the maximum intensities (>IX-X) are mainly grouped in the Capo Vaticano area (indicated with white dots). Here the macroseismic epicenter (the white star) is also located. Some X degrees are located far from the epicentre (see white dots in Fig. 6A). We inverted the 447 intensity data points using the parameters reported in Table 2; the results are shown in the same table. Fig. 8B shows the fault plane solutions resulting from the KF inversion in Table 2; the boxes represent the surface projection of the two modeled sources and the cut-off (thin line) of the hypothesized fault plane with the ground-surface.

Table 2 - Parameters used in the Sant'Eufemia 1905 earthquake inversion.

NGA INVERSION (123 data)	**explored range; step**	**Model 1 (rupture plane) (sub-population 1)**	**Model 2 (sub-population 3)**
PARAMETER		**VALUE ± error**	**VALUE**
Latitude [°] N	±0.35; 0.01	**38.83(±0.06)**	**38.90**
Longitude [°] E	±0.40; 0.01	**16.16(±0.06)**	**16.14**
Strike [°]	0 — 359; 1	**21(±12)**	**110**
Dip [°]	0 — 90; 1	**50(±6)**	**80**
Rake [°]	0 — 180; 1	**270(±6)** (±180)	**-14** (±180)
Depth [km]	6.0 — 24.0; 0.1	**22..9(±1.1)**	**17.0**
Mo [N m 10^{-19}]	1.5 – 6.0; 0.1	**5.18(±2.86)**	**5.50**
Length along strike direction [km]	(*)	**40.0**	**12.0**
Length along anti-strike direction [km]	(*)	**15.0**	**45.0**
Mach along strike direction	0.50 — 0.99; 0.01	**0.85 (±0.11)**	**0.70**
Mach along anti-strike direction	0.50 — 0.99; 0.01	**0.83(±0.09)**	**0.70**
Vs [km sec^{-1}]	3.50 — 3.95; 0.1	**3.79(±0.04)**	**3.38**
Fitness		**258.75**	**273.75**

6. Discussion and conclusions

Based on geophysical data (morpho-bathymetry, Chirp and MCS) that we acquired and studied, we recognized several morphological and tectonic features characterizing the investigated area.

One of the main elements is the MS-High offshore Capo Vaticano, characterized by a very low sedimentation rate on the wide and flat top, and by some gravitational-controlled deformations affecting both flanks of the MS-High. The chaotic sediments that we recognized along its southern side could be interpreted as a slide body, as suggested by (i) deformation of the deposits (Fig. 3B), and (ii) the morphology of the MS-High side (Fig. 2). Unfortunately, the trigger event is not clear, since such slump could be activated and/or controlled by the tectonic activity that contributed to the rise of the MS-High, or by the slope oversteepening along the southern side. The tectonics affecting the MS-High could be associated with the offshore portion of the NFZ (Fig. 1), also called Coccorino Fault (Cucci and Tertulliani, 2010), located south of the Capo Vaticano promontory. The steep slope on the northern side of MS-High borders layered deposits bearing variable thickness, which may have recorded the last tectonic event that affected the MS-High. Comparing the Chirp with the morpho-bathymetric data, we recognized the fault (Fig. 2) along which sedimentary bodies slide, thus generating the steep slope and the small relief (see black arrow) due to the sediments accumulating downslope. The area affected by such fault and its associated gravitational features is about 18 km^2 wide; the fault scarp could be part of a fault

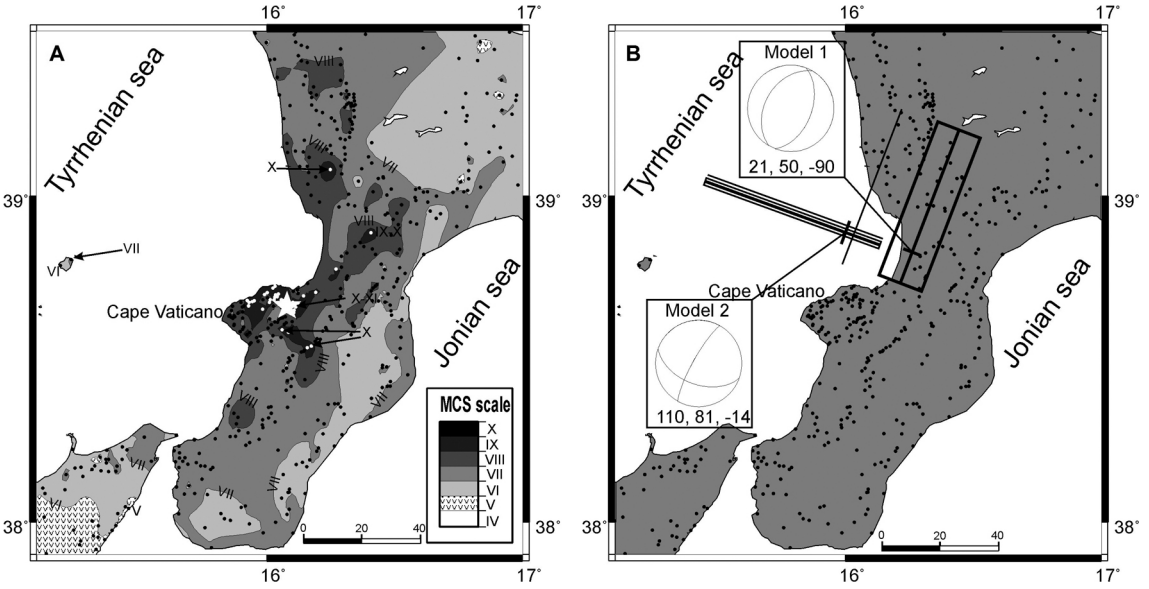

Fig. 8 - September 8, 1905 earthquake: a) observed intensities interpolated using the Natural Neighbor algorithm (Sirovich *et al*., 2002); b) intensities of minimum variance model by KF inversion. The box is the surface projection of the source achieved by inversion. The fault mechanism is on the left side of the picture: a pure dip-slip mechanism, trending NNE-SSW, dipping ESE.

system along which the MS-high was emplaced, as documented by several authors (Dumas *et al*., 1987; Westaway, 1993; Tortorici *et al*., 2003; Cucci and Tertulliani, 2010). Moreover, De Ritis *et al*. (2010) suggest that the MS-High is segmented by a fault system along which magmatic intrusions may have occurred.

SW of the Capo Vaticano promontory, the plumes identified above the lateral discontinuities of present-day sediments (box A1 in Fig. 3A) are interpreted as fluid escape events. The morpho-bathymetric map (see A1 in Fig. 2) reveals an irregularly shaped collapse, corresponding to the deformed sediments (fluid escape zone). Such collapse could be associated with a gravitational slope instability, a slide or debris flow whose inferred slip plane could be due and/or controlled by a weak surface. The latter could be the result of an increase of pore pressure due to an excess of pore fluid trapped below a less permeable layer. The gravitational instability hypothesized is supported by widespread slide and slump morphologies that have been already recognized in the Gioia Tauro Basin (Gamberi *et al*., 2011).

In the Gulf of Sant'Eufemia, morpho-bathymetric data and Chirp profiles have highlighted the presence of a tectonic feature likely controlling the inner segment of the Angitola Channel. Such tectonic control is mainly supported by i) the lateral discontinuity and opposite dipping of shallow sediments at the south-western levee of the channel (Fig. 4), ii) the gentle folding of the Plio-Quaternary sediments below the RB1 (Fig. 6), and iii) several seismic diffractions imaged on the MCS data (Fig. 6). The straight trend of the first 20 km (Fig. 2) of the channel could be controlled by high energy flow currents or by tectonics. Based on the seismic profiles, we deduce that the entire Plio-Quaternary unit (Fig. 6), filling the basin, and the Angitola Channel (Figs. 4

and 6B) could be affected by fault activity – although of unclear kinematics – as shown by the morpho-bathymetric map (Fig. 2).

The hypothesized fault, controlling the Angitola Channel, could be ca. ENE-WSW oriented and located very close to the southern side of the Gulf of Sant'Eufemia (Fig. 2). Using low resolution multichannel seismic profiles, Finetti and Del Ben (1986) identified a regional strike-slip fault called Catanzaro Fault, WNW-ESE oriented, that cross-cuts the external slope and part of the Gulf of Sant'Eufemia. In turn, Tansi *et al*. (2007) defined a complex strike-slip system affecting the Calabrian Arc. Del Ben *et al*. (2008) have also shown major strike-slip systems that may affect the whole eastern sector of the Catanzaro Straits. One of the main faults that belong to such system is the on-land NW-SE oriented Soverato-Lamezia Fault. All the fault systems discussed by the above authors show different orientation with respect to the likely fault affecting the Angitola Channel.

In order to couple geologic information with the damage scenario of the September 8, 1905 earthquake we performed the KF inversion. This procedure returned two possible distinct sources (Fig. 8B) that can be tentatively associated with the 1905 earthquake: i) a dip slip fault, N21° oriented, and ii) a strike-slip fault, N110° oriented. The second one seems to well match the strike-slip fault identified by Finetti and Del Ben (1986), although this is less the case with the Angitola Channel. Whatever the case, the structure that likely controls the Angitola Channel may be either a shallow feature or, in a more complex view, a surface feature that may be in turn controlled by deeper, regional tectonics. However, the anomalous deepening of the Miocene top (white arrow Fig. 7) supports the presence of a structural feature affecting the Angitola Channel, as revealed by the comparison between the Miocene deposits top map and the structures interpreted (solid black line; Fig. 7) or obtained by the KF inversion (red black lines; Fig. 7). The inverted strike-slip case that positively fits the fault identified by Finetti and Del Ben (1986) could be a future work hypothesis.

In turn, the other result of the KF inversion, i.e., the east-dipping dip-slip source, holds interesting potential to be investigated, since its strike recalls that of other large, dip-slip seismogenic sources that lie south of the Gulf of Sant'Eufemia [for a summary, see Basili *et al*. (2008) and DISS Working Group (2010)]. Based on the available data and the current results, the seismogenic source responsible for the 1905 earthquake remains to be clearly identified, thus requiring further analysis of the entire dataset to solve the ambiguity discussed above.

Finally, our data show that the entire upper shelf is affected by intense fluid occurrence, like mud volcanoes and fluid outflows. These features clearly punctuate the otherwise relatively flat seafloor morphology. Moreover, the different depth of the lower unit (U3), measured at the sides of the mud volcano (Fig. 4), and the on-land active tectonics suggests a tectonic control of the upward mud migration. While the different thickness of the U2 unit, measured at both sides of the volcano, could be due to a syn-tectonic deposition of the unit or to a barrier effect of the volcano respect to the water currents transporting sediments. The latter hypothesis implies that the volcano existed during the deposition of the U2 unit. The youngest unit (U1) can be considered a post-tectonic depositional event, as suggested by the sharp truncation of sediments against the mud volcano sides. Such view is supported by the presence of a chaotic deposit at the top of the U2 unit, on the right side (Fig. 5), that could be the result of an erosive event or a mudflow deposit. These elements suggest a multi-history fluid – tectonics interaction. All such

observations, combined with the fluid escape event located south of the MS-High (Fig. 3A) underline that fluid occurrence at the seafloor is strongly controlled by tectonics and closely related to mass-movement.

Given the well known high tectonic complexity of the region and the early stages of the data interpretation, further (i.e., deep-seated) evidence has to be sought before the tectonic features that we have discussed (and subsequent ones that could be identified) can be put in full perspective, particularly in view of the tectonic context which may include the seismogenic source of the September 8, 1905 earthquake (whatever its tectonic expression and kinematics).

Acknowledgments. We wish to thank the Istituto Nazionale di Oceanografia e di Geofisica Sperimentale that supported the acquisition of the entire dataset, with special thanks to R. Ramella, chief of the RIMA Department. Particularly, we thank P. Del Negro for her support on biological data analysis. Moreover, we thank D. Civile, M. Zecchin and D. Ridente for interesting scientific discussions and the two referees for their fruitful comments. Last but not least, we are indebted to the crew of the R/V OGS-Explora for their availability and strong commitment during the cruise.

REFERENCES

Aki K. and Richards P.G.; 1980: *Quantitative seismology. Theory and methods.* W.H. Freeman & Co., San Francisco, 932 pp.

Alvarez W., Cocozza T. and Wezel F.C.; 1974: *Fragmentation of the Alpine orogenic belt by microplate dispersal.* Nature, **248**, 309-314.

Amodio-Morelli L., Bonardi G., Colonna V., Dietrich D., Giunta G., Ippolito F., Liguori V., Lorenzoni P., Paglionico A., Perrone V., Piccarreta G., Russo M., Scandone P., Zanettin-Lorenzoni E. and Zuppetta A.; 1976: *L'Arco Calabro-Peloritano nell'orogene Appenninico-Maghrebide.* Mem. Soc. Geol. It., **17**, 1-60.

Basili R., Valensise G., Vannoli P., Burrato P., Fracassi U., Mariano S. and Tiberti M.M.; 2008: *The Database of Individual Seismogenic Sources (DISS), version 3: summarizing 20 years of research on Italy's earthquake geology.* Tectonophys., **453**, 20-43, doi:10.1016/j.tecto.2007.04.014.

Bigi G., Cosentino D., Parotto M., Sartori R. and Scandone P.; 1992: *Structural Model of Italy, scala 1:500000.* CNR, P.F. Geodinamica, Firenze, sheets 1-6.

Bonardi G., Cavazza W., Perrone V. and Rossi S.; 2001: *Calabria-Peloritani terrane and northern Ionian Sea.* In: Vai G.B. and Martini L.P. (eds), Anatomy of an orogen: the Apennines and adjacent Mediterranean basins, Kluwer, Dordrecht, pp. 287-306.

Boschi E., Ferrari G., Gasperini P., Guidoboni E., Smriglio G. and Valensise G.; 1995: *Catalogo dei forti terremoti in Italia dal 461 a.C. al 1980*. ING-SGA, Bologna, 970 pp.

Camassi R. and Stucchi M.; 1997: *NT 4.1.1, un catalogo parametrico di terremoti di area italiana al di sopra della soglia del danno.* Gruppo Nazionale Difesa dai Terremoti, Rapporto Interno, Milano, 95 pp.

Catalano R. and Sulli A.; 2006: *Crustal image of the Ionian basin and accretionary wedge.* Boll. Geof. Teor. Appl., **47**, 343-374.

Cifelli F., Rossetti F. and Mattei M.; 2007: *The architecture of brittle postorogenic extension: results from an integrated structural and paleomagnetic study in north Calabria (southern Italy).* Geol. Soc. Am. Bull., **119**, 221-239.

Cucci L. and Tertulliani A.; 2010: *The Capo Vaticano (Calabria) coastal terraces and the 1905 M7 earthquake: the geomorphological signature of the regional uplift and coseismic slip in southern Italy*. Terra Nova, **22**, 378-389.

Del Ben A., Barnaba C. and Taboga A.; 2008: *Strike-slip systems as the main tectonic features in the Plio-Quaternary kinematics of the Calabrian Arc.* Mar. Geophys. Res., **29**, 1-12, doi:10.1007/s11001-007-9041-6.

De Ritis R., Dominici R., Ventura G., Nicolosi I., Chiappini M., Speranza F., De Rosa R., Donato P. and Sonnino M.; 2010: *A buried vulcano in the Calabrian Arc (Italy) revealed by high-resolution aeromagnetic data.* J. Geophys. Res., **115**, B11101, doi:10.1029/2009JB007171.

DISS Working Group; 2010: *Database of Individual Seismogenic Sources (DISS), Version 3.1.1: A compilation of potential sources for earthquakes larger than M 5.5 in Italy and surrounding areas.* INGV – Istituto Nazionale di Geofisica e Vulcanologia, http://diss.rm.ingv.it/diss/.

Dumas B., Gueremy P., Lhenaff R. and Raffy J.; 1987: *Rates of uplift as shown by raised Quaternary shorelines in southern Calabria (Italy). Z.* Geomorphol. N.F., **63**, 119-132.

Finetti I. and Del Ben A.; 1986: *Geophysical study of the Tyrrhenian opening*. Boll. Geof. Teor. Appl., **28**, 75-155.

Fracassi U., Di Bucci D., Ridente D., Trincardi F. and Valensise G.; 2012: *Recasting historical earthquakes in coastal areas (Gargano Promontory, Italy): insights from marine paleoseismology*. Bull. Seismol. Soc. Am., **102**, doi:10.1785/0120110001.

Gamberi F. and Marani M.P.; 2004: *Deep-sea depositional systems of the Tyrrhenian Basin*. In: Marani M.P., Gamberi F. and Bonatti E. (eds), From Seafloor to Deep Mantle: Architecture of the Tyrrhenian Backarc Basin, Memorie Descrittive Carta Geologica d'Italia, LXIV, pp. 127-146.

Gamberi F., Rovere M. and Marani M.; 2011*: Mass-transport complex evolution in a tectonically active margin (Gioia Basin, southeastern Tyrrhenian Sea).* Mar. Geol., **279**, 98-110.

Gentile F., Pettenati F. and Sirovich L.; *2004: Validation of the automatic nonlinear source inversion of the U.S. Geological Survey intensities of the Whittier Narrows, 1987 earthquake.* Bull. Seismol. Soc. Am., **94**, 1737-1747.

Gruppo di Lavoro CPTI04; 2004: *Catalogo Parametrico dei Terremoti Italiani, Versione 2004 (CPTI04).* INGV, Bologna, http://emidius.mi.ingv.it/CPTI04/.

Guidoboni E., Ferrari G., Mariotti D., Comastri A., Tarabusi G. and Valensise G.; 2007: *CFTI4Med, Catalogue of Strong Earthquakes in Italy (461 B.C.-1997) and Mediterranean Area (760 B.C.-1500).* INGV-SGA, Bologna, http://storing.ingv.it/cfti4med/.

Levine D.; 1996: *Users guide to the PGAPack parallel genetic algorithm library.* Rep. Argonne National Laboratory, ANL-95/18, Argonne, IL, 73 pp.

Mattei M., Cipollari P., Casentino D., Argentieri A., Rossetti F. and Speranza F.; 2002: *The Miocene tectonic evolution of the Southern Tyrrhenian Sea: stratigraphy, structural and paleomagnetic data from the on-shore Amantea basin (Calabrian Arc, Italy).* Basin Res., **14**, 147-168.

Michelini A., Lomax A., Nardi A. and Rossi A.; 2006: *La localizzazione del terremoto della Calabria dell'8 settembre 1905 da dati strumentali.* In: Guerra I. and Savaglio A. (eds), 8 settembre 1905: terremoto in Calabria, Università della Calabria, pp. 225-240.

Milia A., Turco E., Pierantoni P.P. and Schettino A.; 2009: *Four-dimensional tectonostratigraphic evolution of the Southern peri-Tyrrhenian basins (margin of Calabria, Italy).* Tectonophys., **476**, 41-56, doi:10.1016/j.tecto.2009.02.030.

Pepe F., Sulli A., Bertotti G. and Cella F.; 2010: *Architecture and Neogene to Recent evolution of the western Calabrian continental margin: An upper plate perspective to the Ionian subduction system, central Mediterranean.* Tectonics, **29**, TC3007, doi:10.1029/2009TC002599.

Pettenati F. and Sirovich L.; 2003: *Test of source inversion of the USGS "Felt Reports" of the Whittier Narrows, 1987 earthquake.* Bull. Seismol. Soc. Am., **93,** 47-60.

Pettenati F. and Sirovich L.; 2007: *Validation of intensity-based source inversion of three destructive Californian Earthquakes.* Bull. Seismol. Soc. Am., **97**, 1587-1606, doi:10.1785/0120060169.

Pettenati F., Sirovich L., Bungum H. and Schweitzer J.; 2005: *Source inversion of regional intensity patterns of five earthquakes from south-western Norway.* Boll. Geof. Teor. Appl., **46**, 111-134.

Piatanesi A. and Tinti S.; 2002: *Numerical modelling of the September 8, 1905 Calabrian (southern Italy) tsunami.* Geophys. J. Int., **150**, 271-284, doi:10.1046/j.1365-246X.2002.01700.x.

Pirazzoli P.A., Mastronuzzi G., Saliège J.F. and Sansò P.; 1997: *Late Holocene emergence in Calabria, Italy.* Mar. Geol., **141,** 61-70, doi:10.1016/S0025- 3227(97)00057-1.

Riuscetti M. and Schick R.; 1974: *Earthquakes and tectonics in southern Italy.* In: Proc. Joint Symp. Eur. Seismol. Comm. and Eur. Geophys. Sco., Trieste, Italy, September 21, pp. 59-78.

Rizzo G.B.; 1906: *Sulla velocità di propagazione delle onde sismiche del terremoto della Calabria del giorno 8 Settembre 1905.* Mem. R. Accad. Sci., Torino, 1905-1906, s. II, Tom. LVII.

Sartori R.; 1990: *The main results of ODP Leg 107 in the frame of Neogene to recent geology of peri-Tyrrhenian areas.* In: Kastens K.A. *et al.* (eds), Proc. Ocean Drill. Program, Sci. Results, 107 College Station, pp. 715-730.

Sartori R.; 2003: *The Tyrrhenian back-arc basin and subduction of the Ionian lithosphere*. Episodes, **26,** 217-221.

Sirovich L.; 1996: *A simple algorithm for tracing out synthetic isoseismals.* Bull. Seismol. Soc. Am., **86**, 1019-1027.

Sirovich L. and Pettenati F.; 2004: *Source inversion of intensity patterns of earthquakes: a destructive shock in 1936 in northern Italy.* J. Geophys. Res., **109**, B10309, doi:10.1029/2003JB002919.

Sirovich L., Pettenati F., Cavallini F. and Bobbio M.; 2002: *Natural-Neighbor Isoseismals.* Bull. Seismol. Soc. Am., **92**, 1933-1940.

Tansi C., Muto F., Critelli S. and Iovine G.; 2007: *Neogene - Quaternary strike-slip tectonics in the central Calabrian Arc (Southern Italy).* J. Geodyn., **43**, 393-414.

Tertulliani A. and Cucci L.; 2009: *Clues to the identification of a seismogenic source from environmental effects: the case of the 1905 Calabria (Southern Italy) earthquake.* Nat. Hazards Earth Syst. Sci., **9**, 1787-1803, doi:10.5194/nhess-9-1787-2009.

Tiberti M.M., Fracassi U. and Valensise G.; 2006*: Il quadro sismotettonico del grande terremoto del 1905.* In: Guerra I. and Savaglio A. (eds), 8 Settembre 1905: terremoto in Calabria, Università della Calabria, pp. 181-205.

Tortorici G., Bianca M., De Guidi G., Monaco C. and Tortorici L.; 2003: *Fault activity and marine terracing in the Capo Vaticano area (southern Calabria) during the Middle-Late Quaternary.* Quat. Int., **101-102**, 269-278.

Van Dijk J.P., Bello M., Brancaleoni G.P., Cantarella G., Costa V., Frixa Golfetto F., Merlini S., Riva M., Torricelli S., Toscano C. and Zerilli A.; 2000: *A regional strucutral model for the northern sector of the Calabrian Arc (southern Italy).* Tectonophys., **324**, 267-320.

Westaway R.; 1993: *Quaternary uplift of Southern Italy.* J. Geophys. Res., **98**, 21741-21772.

Corresponding author: Maria Filomena Loreto
Istituto Nazionale di Oceanografia e di Geofisica Sperimentale
Borgo Grotta Gigante 42/c, 34010 Sgonico (Trieste), Italy
Phone: +39 040 2140305; fax: +39 040 327307; e-mail: mloreto@inogs.it